Received: 15 July 2020 | Accepted: 11 November 2020

DOI: 10.1002/pamm.202000234

Extension of an analytical solution of a unified formulation to the frequency response of composite plates with viscoelastic layers

Alexander Jackstadt[1,*] and **Luise Kärger**[1]

[1] Karlsruhe Institute of Technology (KIT), Institute of Vehicle System Technology, Rintheimer Querallee 2, 76131 Karlsruhe, Germany

Resulting from their high stiffness and low weight, lightweight structures made from fiber reinforced polymers are usually prone to vibrations. The inclusion of viscoelastic interlayers can provide a viable mean to passively damp these structures due to constrained layer damping. For the modeling of such structures, a layerwise approach based on the Generalized Unified Formulation has previously been proven suitable for static load cases.

This contribution presents an analytical procedure to determine the frequency response and vibration characteristics of such heterogeneous laminates incorporating viscoelastic layers. Specifically, simply supported plates modeled by the Generalized Unified Formulation are considered and solved using Navier type solutions. The approach is validated by comparison with 3D finite element models. Particular focus is put on the order of expansion in thickness direction needed to accurately predict the frequency response of the laminate.

1 Introduction

As lightweight structures can be prone to vibrations due to their usually high stiffness and low weight, intrinsic material damping can be used to damp these unwanted oscillations. One of these intrinsic damping mechanisms is constrained-layer damping where a viscoelastic and compliant layer is laminated in between two stiff constraining layers. The under bending induced large transverse shear deformations in the constrained viscoelastic middle layer lead to the dissipation of vibration energy. Knowledge of the transverse deformations in the constrained layer is crucial in the design of such damped laminates. In a previous publication [1], the authors have introduced an analytical procedure based on a layerwise plate theory according to the Generalized Unified Formulation (GUF) published by Demasi [2] for the static strain and stress analysis able to cope with the highly heterogeneous stiffness distribution in such hybrid laminates.

In this work, the previously developed analytical procedure based on Navier type solutions is extended by incorporating the viscoelastic material behavior of elastomer damping layers within the GUF framework and determine the damped frequency response. A similar procedure has been developed by Alaimo et al. [3] for a different set of layerwise plate theories based on the principle of virtual displacements (PVD). In this work, however, theories based on the Reissner's mixed variational theorem (RMVT) are considered as they provide better approximations of out-of-plane stresses.

2 Method

2.1 Variational formulation and plate kinematics

In this work, the RMVT shown in Eqn. (1) is considered due to its suitability in modeling the transverse stresses crucial in constrained layer damping applications.

$$\int_\Omega \left(\delta\boldsymbol{\varepsilon}_{\mathrm{pG}}^\top\boldsymbol{\sigma}_{\mathrm{pH}} + \delta\boldsymbol{\varepsilon}_{\mathrm{nG}}^\top\boldsymbol{\sigma}_{\mathrm{nM}} + \delta\boldsymbol{\sigma}_{\mathrm{nM}}^\top\left(\boldsymbol{\varepsilon}_{\mathrm{nG}} - \boldsymbol{\varepsilon}_{\mathrm{nH}}\right)\right)\mathrm{d}V = \delta L_{\mathrm{external}} + \int_\Omega \rho\delta\boldsymbol{u}\ddot{\boldsymbol{u}}\mathrm{d}V \tag{1}$$

Index n in Eqn. (1) denotes out-of-plane quantities, whereas p stands for in-plane. Quantities which are explicitly modeled are denoted by M. The remaining components in Eqn. (1) are either calculated from the displacements by geometric relations (index G) or calculated using the constitutive law (index H). L_{external} is the external virtual work. The last term in Eqn. (1) containing the acceleration vector $\ddot{\boldsymbol{u}}$ presents the contribution of inertia. In each laminate layer k, the three displacements u_x^k, u_y^k and u_z^k as well as the three out-of-plane stresses σ_{xz}^k, σ_{yz}^k and σ_{zz}^k are modeled as

$$\begin{aligned}
u_x^k(x,y,z) &= U_{x,\alpha_{u_z}}^k F_{\alpha_{u_z}}(z)\Phi_{u_x}(x,y), \quad \sigma_{xz}^k(x,y,z) = S_{xz,\alpha_{\sigma_{xz}}}^k F_{\alpha_{\sigma_{xz}}}(z)\Phi_{\sigma_{xz}}(x,y),\\
u_y^k(x,y,z) &= U_{y,\alpha_{u_y}}^k F_{\alpha_{u_y}}(z)\Phi_{u_y}(x,y), \quad \sigma_{yz}^k(x,y,z) = S_{yz,\alpha_{\sigma_{yz}}}^k F_{\alpha_{\sigma_{yz}}}(z)\Phi_{\sigma_{yz}}(x,y),\\
u_z^k(x,y,z) &= U_{z,\alpha_{u_z}}^k F_{\alpha_{u_z}}(z)\Phi_{u_z}(x,y), \quad \sigma_{zz}^k(x,y,z) = S_{zz,\alpha_{\sigma_{zz}}}^k F_{\alpha_{\sigma_{zz}}}(z)\Phi_{\sigma_{zz}}(x,y)
\end{aligned} \tag{2}$$

* Corresponding author: e-mail alexander.jackstadt@kit.edu, phone +49 721 608 45365

according to the GUF framework. The in-plane dependencies are summarized by the functions $\Phi(x, y)$ which will be provided by the chosen solution method. For reasons of brevity, the reader is referred to the original publications by Demasi [2, 4] and a previous work of the authors [1] for more details on the expansions of the thickness functions $F(z)$ and the assembly of the global system of equations.

2.2 Solution method for frequency response

In order to account for frequency dependent viscoelastic material behavior, the constitutive relations are specified dependent on the complex shear modulus $G^* = \Re(G^*) + \mathrm{i}\Im(G^*) = G' + \mathrm{i}G''$, where i denotes the imaginary number. This leads to consequent quantities also being complex. A simply supported plate problem as shown in Fig. 1 is considered in the following and the solution is obtained using the Navier method, illustrated amongst others in Reddy [5], and extended to yield the plate's frequency response to forced vibration. First, a general harmonic load

$$q(x, y, t) = \hat{q}(x, y)\mathrm{e}^{\mathrm{i}\omega t} \tag{3}$$

is applied to the topmost layer of the plate. An analytical solution is obtained using the Navier method by expanding the pressure load $q(x, y)$ as a double trigonometric series

$$\hat{q}(x, y) = \sum_{m=1}^{\infty}\sum_{n=1}^{\infty} Q_{mn} \sin\left(\frac{m\pi}{a}x\right)\cos\left(\frac{n\pi}{b}y\right) \approx \sum_{m=1}^{M}\sum_{n=1}^{N} Q_{mn} \sin\left(\frac{m\pi}{a}x\right)\cos\left(\frac{n\pi}{b}y\right) \tag{4}$$

which is approximated by an expansion up to orders M and N. The load coefficient Q_{mn} in Eqn. (4) for the concentrated force shown in Fig. 1 is defined as

$$Q_{mn} = \frac{4Q_0}{ab}\sin(\frac{m\pi}{a}x_0)\sin(\frac{n\pi}{b}y_0) \tag{5}$$

when applied at coordinates x_0 and y_0. Following the assumptions made for the load, the problem's solution is also a superposition of M respectively N closed solutions. Displacement and out-of-plane stress amplitudes are thus calculated as

$$\begin{aligned}
\hat{u}_x^k(x, y, z) &\approx \sum_{m=1}^{M}\sum_{n=1}^{N} U_{x,\alpha_{u_x}}^{k,mn} F_{\alpha_{u_x}}(z)\cos\left(\frac{m\pi}{a}x\right)\sin\left(\frac{n\pi}{b}y\right),\\
\hat{u}_y^k(x, y, z) &\approx \sum_{m=1}^{M}\sum_{n=1}^{N} U_{y,\alpha_{u_y}}^{k,mn} F_{\alpha_{u_y}}(z)\sin\left(\frac{m\pi}{a}x\right)\cos\left(\frac{n\pi}{b}y\right),\\
\hat{u}_z^k(x, y, z) &\approx \sum_{m=1}^{M}\sum_{n=1}^{N} U_{z,\alpha_{u_z}}^{k,mn} F_{\alpha_{u_z}}(z)\sin\left(\frac{m\pi}{a}x\right)\sin\left(\frac{n\pi}{b}y\right),\\
\hat{\sigma}_{xz}^k(x, y, z) &\approx \sum_{m=1}^{M}\sum_{n=1}^{N} S_{xz,\alpha_{\sigma_{xz}}}^{k,mn} F_{\alpha_{\sigma_{xz}}}(z)\cos\left(\frac{m\pi}{a}x\right)\sin\left(\frac{n\pi}{b}y\right),\\
\hat{\sigma}_{yz}^k(x, y, z) &\approx \sum_{m=1}^{M}\sum_{n=1}^{N} S_{yz,\alpha_{\sigma_{yz}}}^{k,mn} F_{\alpha_{\sigma_{yz}}}(z)\sin\left(\frac{m\pi}{a}x\right)\cos\left(\frac{n\pi}{b}y\right),\\
\hat{\sigma}_{zz}^k(x, y, z) &\approx \sum_{m=1}^{M}\sum_{n=1}^{N} S_{zz,\alpha_{\sigma_{zz}}}^{k,mn} F_{\alpha_{\sigma_{zz}}}(z)\sin\left(\frac{m\pi}{a}x\right)\sin\left(\frac{n\pi}{b}y\right)
\end{aligned} \tag{6}$$

from the solution vectors $\boldsymbol{U}^{mn}$ containing the layerwise displacements $U_{i,\alpha_{u_i}}^{k,mn}$ and transverse stresses $S_{iz,\alpha_{\sigma_{iz}}}^{k,mn}$ of the global systems of equations

$$\left(\boldsymbol{K}^* - \omega^2\boldsymbol{M}\right)\boldsymbol{U}^{*^{mn}} = \boldsymbol{R}. \tag{7}$$

3 Application

3.1 Example problem

This method is illustrated by considering the simply supported laminated plate in Fig. 1 consisting of an elastomer layer constrained by two aluminum sheets and subjected to a harmonic concentrated force in the center of the top layer. The plate's dimensions are listed in Tab. 1. The aluminum is modeled as linear elastic with the parameters in Tab. 2. The viscoelastic elastomer is modeled using the complex modulus approach with interpolation of the experimental data shown in Fig. 2.

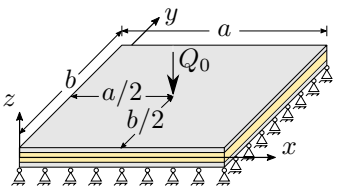

Fig. 1: Simply supported plate problem subjected to a concentrated force Q_0. The gray layers are aluminum whereas yellow indicates the elastomer layer.

Table 1: Parameters of plate problem corresponding to Fig. 1.

a	b	$\lvert Q_0 \rvert$	t_{Aluminum}	$t_{\text{Elastomer}}$
0.4 m	0.4 m	100 N	0.3 mm	0.5 mm

Table 2: Mechanical properties of constituents such as density ρ, Young's modulus E and Poisson's ratio ν. No Young's modulus is listed for the elastomer material due to its frequency dependency. In this study, the Young's modulus at a given frequency is calculated from the complex shear modulus shown in Fig. 2.

Material	ρ	E	ν
Elastomer	$1.18 \times 10^3\,\mathrm{kg\,m^{-3}}$	-	0.48
Aluminum	$2.78 \times 10^3\,\mathrm{kg\,m^{-3}}$	$73.1 \times 10^3\,\mathrm{MPa}$	0.3

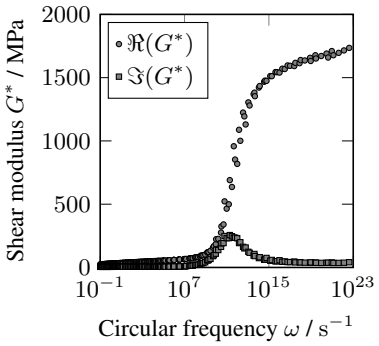

Fig. 2: Complex shear modulus of elastomer material taken from Sessner et al. [6].

First, a convergence study is conducted in order to determine how many terms in the Fourier series in Eqn. (4) need to be expanded for acceptable accuracy. Since the plate is quadratic and isotropic, only expansions with $M = N$ are considered. The results are then compared with the solution provided by a 3D Finite Element Method (FEM) steady-state analysis in Abaqus using the same material parameters and boundary conditions. The absolute deflection amplitude in the center of the plate $|\hat{u}_z^*(x = \frac{a}{2}, y = \frac{b}{2}, z = \frac{h}{2})|$ is investigated as well as the phase angle δ calculated as the counterclockwise angle between the real and imaginary part of the deflection $\hat{u}_z^*(x = \frac{a}{2}, y = \frac{b}{2}, z = \frac{h}{2})$. For the circular frequency ω a range of 1 to $3000\,\mathrm{s}^{-1}$ is considered. Furthermore, different layerwise theories are investigated, namely theories LW_{111}^{333}, LW_{113}^{333} and LW_{333}^{555}. The theories are compared using a series expansion of $M = N = 32$ and validated against the aforementioned 3D FEM results.

3.2 Results

The results of the convergence study can be seen in in Fig. 3. An expansion up to order $M = N = 64$ is shown as higher orders of expansions have yielded identical results. In the left graph showing the transverse displacement magnitude $|\hat{u}_z^*|$, the FEM solution is plotted and the four resonance frequencies in the given frequency spectrum can be identified by their high amplitudes. It can be seen, that an series expansion of order $M = N = 1$ depicts well the first resonance frequency but is unable to reproduce the higher modes. An expansion of order $M = N = 4$ captures the first three resonance frequencies whereas all subsequent higher expansions depict all four modes, however with varying accuracy between resonances. The graph on the left in Fig. 3 displays the phase angle δ with which the structural response lags behind the excitation. Again, resonances are depicted well by expansions higher than $M = N = 4$ in the given frequency range. Furthermore, the increased damping of higher modes is visible by the sloped phase angle curve when passing $90°$. The comparison of different layerwise theories in Fig. 4 shows that the results of all theories considered coincide save some minor discrepancies. It can be seen that the analytical solutions differ from the FEM results by an increasing horizontal shift for higher frequencies. The amplitudes in the resonance peaks, however, correspond well with the FEM results. These observations are true for both, the displacement magnitude $|\hat{u}_z^*|$ and the phase angle δ.

3.3 Discussion

The results outlined above show that the developed analytical procedure is well capable of predicting the frequency response of simply supported plates. The order of expansion of the trigonometric series, however, needs to be high enough to depict the kinematics of the respective vibration modes in the analyzed frequency range. For the given test case, an expansion of $M = N = 64$ has been identified as a convergence limit with lower expansion orders of $M = N = 32$ leading to neglectable deviations. This also agrees with the findings of Alaimo et al. [3] who also studied the influence of plates' aspect ratios on the convergence. The investigation of different layerwise theories has shown that theory LW_{111}^{333} with a linear approach for displacements and a cubic expansion for out-of-plane stresses yields the results as close to the FEM solution as the higher

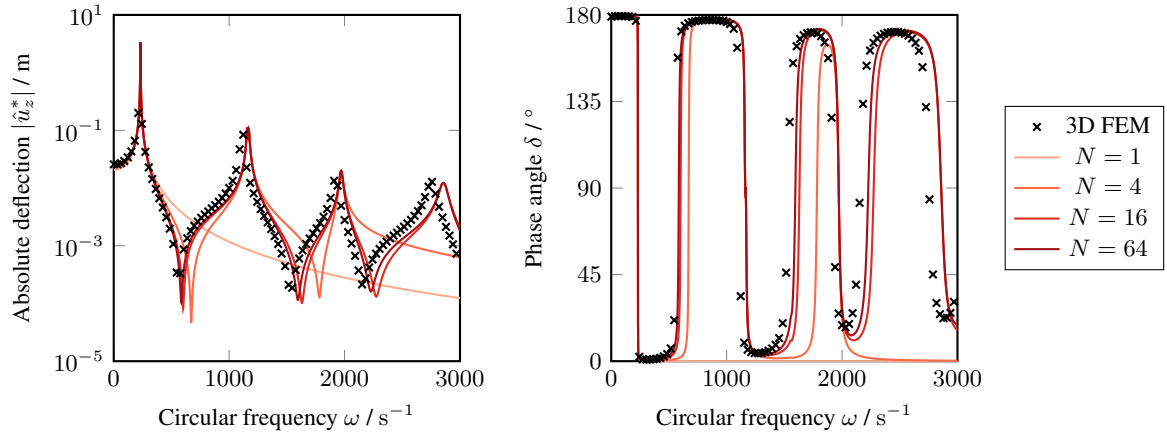

Fig. 3: Convergence study on order N of Fourier series expansion with regard to the absolute magnitude of transverse deflection $|\hat{u}_z^*|$ in transverse direction (left) and the corresponding phase angle δ (right).

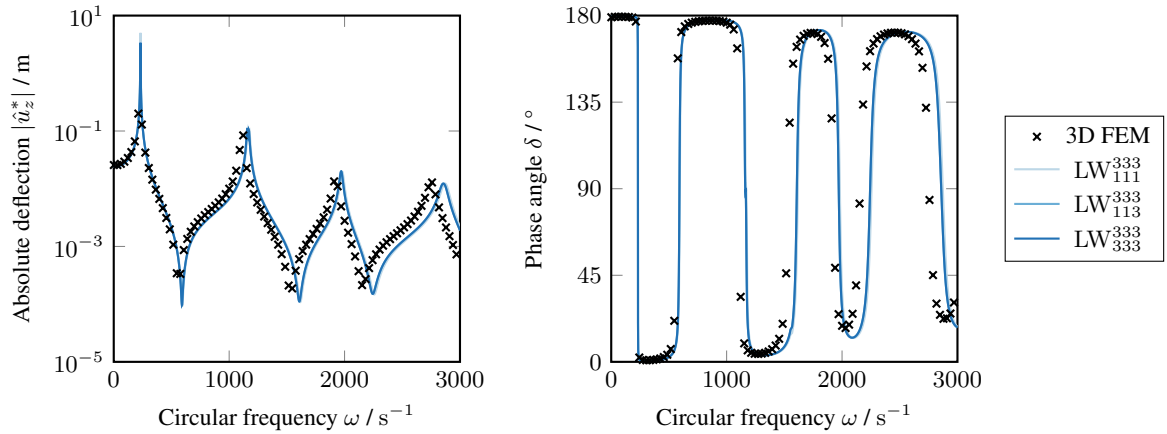

Fig. 4: Transverse displacement magnitudes and phase angles for different layerwise theories.

order theories also investigated. The deviations of the analytical solution with respect to the FEM reference solution could be attributed to using a different variational theorem or the difference in the kinematic approach.

4 Conclusion

In this work, an analytical solution method has been developed for the analysis of the damped frequency response of simply supported plates including viscoelastic layers based on the RMVT by using the GUF framework. Very good agreement with a FEM reference solution is achieved. This method provides a valuable tool in evaluating the damping capabilities of constrained layer laminates and, due to its minimal computation effort, allows for rapid design and optimization of specific laminate layups.

Acknowledgements This work is funded by the Deutsche Forschungsgemeinschaft (DFG, German Research Foundation) SPP1897 “Calm, Smooth, Smart – Novel approaches for influencing vibrations by means of deliberately introduced dissipation”, project KA 4224/3-2 “HyCEML – Hybrid CFRP/elastomer/metal laminates containing elastomeric interfaces for deliberate dissipation” (Karlsruhe Institute of Technology). The work is also part of the Young Investigator Group (YIG) “Green Mobility”, generously funded by the Vector Stiftung. Open access funding enabled and organized by Projekt DEAL.

References

[1] A. Jackstadt, W. V. Liebig, V. Sessner, K. A. Weidenmann, and L. Kärger, PAMM **19**(1), e201900048 (2019).
[2] L. Demasi, Composite Structures **87**(1), 12–22 (2009).
[3] A. Alaimo, C. Orlando, and S. Valvano, Aerospace Science and Technology **92**, 429–445 (2019).
[4] L. Demasi, Composite Structures **87**(1), 1–11 (2009).
[5] J. N. Reddy, Mechanics of Laminated Composite Plates and Shells (CRC Press, Boca Raton, FL, 2004).
[6] V. Sessner, A. Jackstadt, W. V. Liebig, L. Kärger, and K. A. Weidenmann, Journal of Composites Science **3**(1), 3 (2019).

